

Gas-assisted exfoliation of boron nitride nanosheets enhancing adsorption performance



Yanhong Chao^a, Mei Liu^a, Jingyu Pang^{b,c,*}, Peiwen Wu^c, Yan Jin^a, Xiaowei Li^c, Jing Luo^c, Jun Xiong^c, Huaming Li^c, Wenshuai Zhu^{c,**}

^a School of Pharmacy, Jiangsu University, Zhenjiang, 212013, PR China

^b College of Chemistry and Chemical Engineering, Henan Engineering Research Center of Industrial Circulating Water Treatment, Henan University, Kaifeng, 475004, PR China

^c School of Chemistry and Chemical Engineering, Jiangsu University, Zhenjiang, 212013, PR China

ARTICLE INFO

Keywords:

Boron nitride
Adsorption
Gas exfoliation
Organic contaminants

ABSTRACT

A gas exfoliation strategy for controllable preparation of boron nitride (BN) nanosheets with few-layered structure were reported. The green exfoliation process provides the BN nanosheets remarkable increment of adsorption capacities to organic contaminants, which is ascribed to better exposure of active sites originating from the larger surface area and thinner layer. Moreover, the prepared BN also exhibits outstanding recyclability.

1. Introduction

In recent years, water pollution has turned to be a widespread problem with the development of industry and agriculture [1,2]. Organic contaminants in wastewater, such as dyes [3–5] and antibiotics [6,7], may cause significant health problems and environmental pollution. Therefore, efficient removal of organic contaminants from wastewater is a crucial topic for the environment. Currently, adsorption [8–10] has been proved to be an efficient process. Developing novel adsorbents with high adsorption capacity and simple synthesis process is of critical importance.

Hexagonal boron nitride (*h*-BN) nanosheet is known as white graphene with alternating boron and nitrogen atoms arranged in a hexagonal structure [11–13]. The unique properties [14–16], such as superior thermal stability, oxidation resistance and excellent mechanical strength, drive it to be an ideal candidate for the adsorption process. However, the bulk BN suffers from the low specific surface area (SSA) and poor exposure of active sites, making it holds less satisfying adsorption capacity to organic contaminants. Thusly, mechanical cleavage [17–19] and liquid-phase [20–22] exfoliation have been developed to overcome the disadvantage. However, these processes are time-consuming, ungreen, and the yield is low. Therefore, designing a simple, green, scalable method without using chemical solutions remains a challenge. Recently, gas exfoliation has been developed by our group as

a simple and green strategy for the fabrication of few-layered 2D materials [23,24]. It was proved to be an efficient method without using chemical solutions for the production of few-layered nanosheets on large scale.

In this study, fewer-layered boron nitride nanosheets were successfully designed and prepared by such green gas exfoliation strategy. The as-prepared 2D nanomaterials showed promising performance for the rapid removal of tetracycline (TC), gatifloxacin (GT), rhodamine B (RhB) and methylene blue (MB) from aqueous with excellent reusability. The gas exfoliation approach offered an idea for the efficient design of 2D materials as promising adsorbents for effective water-treatment.

2. Experimental

2.1. Material

Commercial hexagonal boron nitride (*h*-BN, lateral size 1–10 μm) was purchased from Sigma-Aldrich. Other reagents and solutions were derived from Sinopharm Chemical Reagent without further purification. Liquid nitrogen (L-N₂) was supplied by Suzhou Jinhong Co., Ltd (China).

* Corresponding author. .

** Corresponding author. .

E-mail addresses: pjy@henu.edu.cn (J. Pang), zhuws@ujs.edu.cn (W. Zhu).

<https://doi.org/10.1016/j.ceramint.2019.06.117>

Received 5 April 2019; Received in revised form 11 June 2019; Accepted 12 June 2019

Available online 21 June 2019

0272-8842/© 2019 Elsevier Ltd and Techna Group S.r.l. All rights reserved.

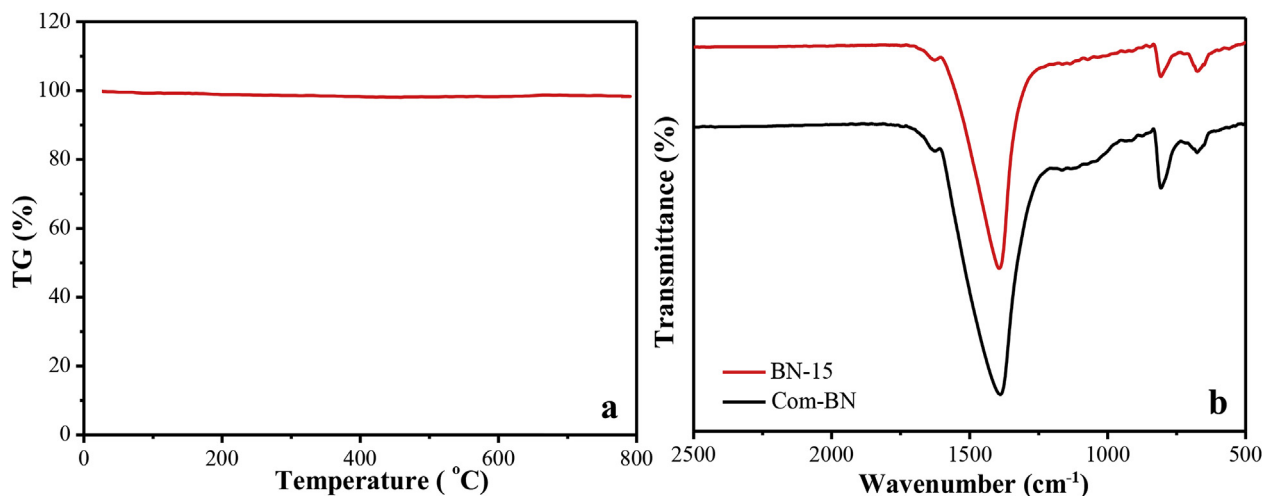


Fig. 1. (a) TGA of Com-BN in air; (b) FTIR spectra of Com-BN and BN-15.

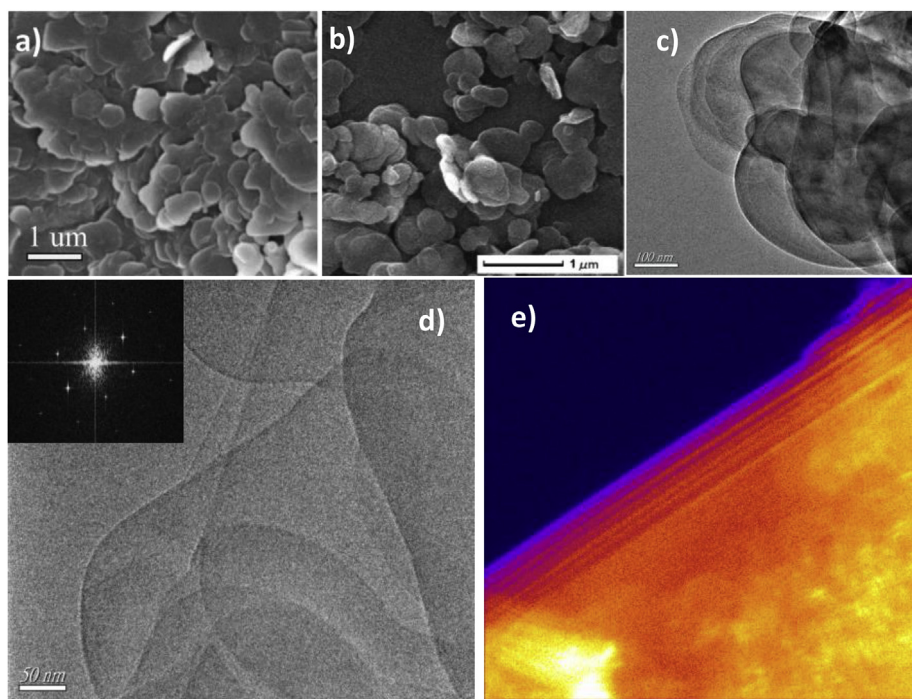


Fig. 2. SEM images of Com-BN (a) and BN-15 (b); TEM images of Com-BN (c) and BN-15 (d); STEM images of BN-15 (e).

2.2. Fabrication of few-layer BN

Commercial BN (Com-BN, 1.0 g) was heated at 800 °C for 8 min in a muffle furnace under air atmosphere. Afterwards, the high-temperature heated Com-BN was transferred into the polytetrafluoroethylene beaker filled with liquid nitrogen (L-N₂) and vibrated till the L-N₂ gasified completely. Then the solid powers were collected for the next cycle. The above steps were repeated 15 cycles. Subsequently, the sample was sonicated in ethanol for 0.5 h. Then the products were centrifuged at 1000 rpm for 10 min to remove un-exfoliated bulk component. The supernatant was concentrated and dried in vacuum overnight. Then few-layer BN were achieved and marked as BN-15.

2.3. Characterization

FT-IR and Raman spectra were conducted on Nexus 470 (Thermo Electron Corporation) and DXR Raman microscope (Renishaw Invia,

using 532 nm as an excitation source). The crystal phase characteristics were recorded by powder X-ray diffraction using Bruker D8 diffractometer (CuK α). Thermogravimetric analysis (TGA) was done on STA-449C Jupiter (NETZSCH Corporation, Germany). The sample was tested from room temperature to 800 °C with a heating rate of 10 °C/min under air atmosphere with 60 L/min of air flowing. Morphology was observed through scanning electron microscopy (JEOL JSM-7001F) and transmission electron microscopy (JEOL JEM-2100). Atomic force microscopy (AFM) was used to analyze interlayer information of materials by Asylum MFP-3D (Asylum Research Company). Brunauer-Emmett-Teller (BET) method studies were carried out by Quadrasorb SI (Quantachrome, USA).

2.4. Adsorption activity measurement

The adsorption performances of BN sample for organic pollutants of tetracycline (TC), gatifloxacin (GT), rhodamine B (RhB) and methylene

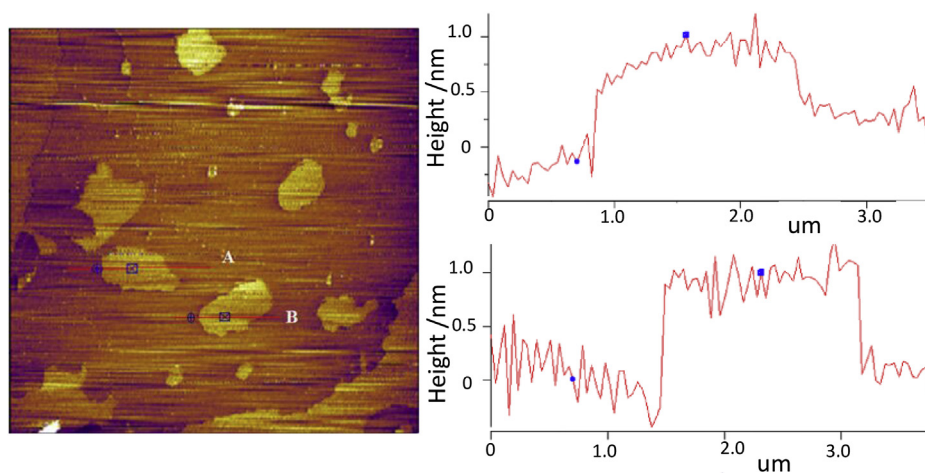


Fig. 3. AFM image and the corresponding height profiles of BN-15.

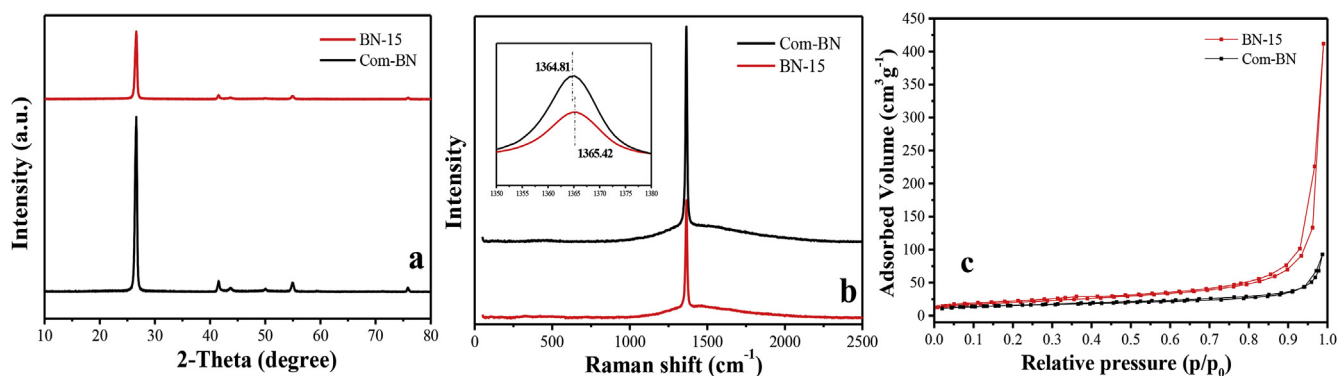


Fig. 4. (a) XRD patterns, (b) Raman spectra, (c) Nitrogen adsorption-desorption isotherms of BN-15 and Com-BN.

blue (MB) were evaluated with batch adsorption experiments. In a typical adsorption experiment, 5 mg of adsorbents were added in 25 mL of TC solutions with concentration of 100 ppm and initial pH of 3.58. Then the mixtures were shaken in a thermostatic water bath for a period of time to reach adsorption equilibrium. The concentration of TC was determined by a UV–vis spectrophotometer (UV-2501) based on the standard curve after filtration. The other adsorption experiments were operated in the same conditions but different organic pollutants of GT (pH 7.44), RhB (pH 3.95), MB (pH 5.42), respectively. The adsorption capacity (q_t , mg/g) was calculated on the basis of Eq. (1).

$$q_t = \frac{(C_0 - C_t)V}{m} \quad (1)$$

where C_0 and C_t are the initial and the t time concentrations of organic pollutants in the test solution (mg/L), V is the volume of the solution (L), and m is the weight of the adsorbent (g).

3. Results and discussion

To investigate the thermal stability of BN, TGA was measured under air atmosphere (Fig. 1a). With the increasing of temperature, no obvious weight loss was found in TGA curve. IR was employed to contrast the chemical structure of BN samples after exfoliation. The results were showed in Fig. 1b, the peaks at 804 cm^{-1} and 1387 cm^{-1} were ascribed to the stretching vibration of B–N and out-plan bending vibration of B–N–B, respectively [25,26]. Both of the analysis indicated that the physical and chemical structures were stable after high temperature processing.

The morphology of BN-15 was illustrated via SEM and TEM (Fig. 2). Compared with the initial Com-BN, the BN-15 held a smaller size and

thinner morphology. As shown in Fig. 2d, BN-15 exhibited an obvious stack structure, and the inset in Fig. 2d showed the corresponding typical hexagonal symmetry electron diffraction structure of BN-15 [27]. A STEM image was shown in Fig. 2e, which exhibited a representative terraced few-layered structure.

The height variation of surface profiles for the prepared BN-15 was further characterized by AFM. Numerous nanosheets with diameters of 0–1 μm can be clearly seen in the AFM image (Fig. 3). The thickness of the BN-15 was also found to be few-layered structure, and the minimum thickness was about 1.1 nm. This result agreed with STEM characterization. For comparison, the thickness of Com-BN was further determined by AFM in Fig. S1 and the thickness was found to be 25–42 nm, further proving that the gas exfoliation strategy decreased the thickness of bulk BN remarkably.

The crystal and chemical structures of BN-15 were investigated by XRD and Raman spectra. As shown in the XRD patterns in Fig. 4a the intensity of (002) peak decreased significantly after exfoliation. The obvious change in XRD spectra resulted from the reduction of ordered stacking in the c direction [28]. This is consistent with the results in SEM and TEM. The Raman spectra (Fig. 4b) showed that the E_{2g} mode of BN-15 shifted to 1365.42 cm^{-1} compared to Com-BN (1364.81 cm^{-1}). The slight change indicates the reduction of interlayer interaction and the enhancement of in-plane strain after exfoliation [29]. Furthermore, the full width half maximum (FWHM) of BN-15 (16.61 cm^{-1}) was broader than that of com-BN (15.76 cm^{-1}), suggesting the decrease of the thickness of BN [30].

The N_2 adsorption-desorption isotherms were shown in Fig. 4c. The few-layered BN-15 nanosheets possessed of much larger SSA ($\sim 101 \text{ m}^2/\text{g}$) than that of Com-BN ($\sim 20 \text{ m}^2/\text{g}$) because of the decrease of thickness. Besides, the much thinner BN-15 could expose more active

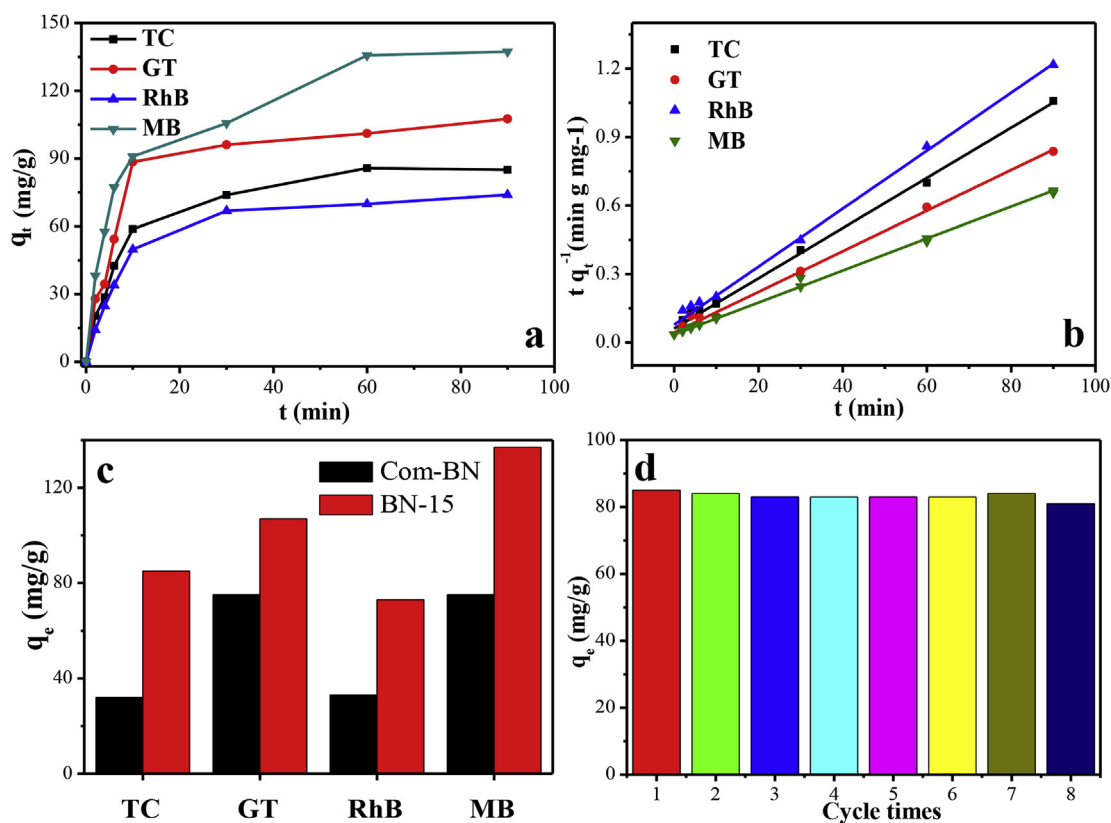


Fig. 5. (a) The effect of contact time, (b) the plots of the pseudo-second-order kinetic model, (c) the adsorption capacities of different organic pollutants onto the as-prepared BN-15, and (d) the reusability of BN-15. (Condition: $C_0 = 100$ mg/L; $T = 298$ K; $m = 5$ mg; $V = 10$ mL; $pH_{TC} = 3.58$, $pH_{GT} = 7.44$, $pH_{RhB} = 3.95$, $pH_{MB} = 5.42$).

Table 1

Kinetic parameters for different organic pollutants adsorption onto BN-15.

	Pseudo-first order			Pseudo-second order			
	q_e (mg/g)	K_1 (min ⁻¹)	R^2	q_e (mg/g)	$t_{1/2}$ (min)	K_2 (g*mg ⁻¹ min ⁻¹)	R^2
TC	61	0.032	0.88	91	5.58	0.0020	0.99
GT	69	0.033	0.88	112	4.94	0.0018	0.99
RhB	54	0.029	0.90	79	6.19	0.0021	0.99
MB	98	0.035	0.94	143	5.09	0.0014	0.99

edge sites [31] for enhanced adsorption performance. The SSA of BN-15 nanosheet is lower than that of the previous work [23], which may lie in the different precursor of Com-BN.

The mechanism of the L-N₂ gas exfoliation had been discussed as follows: According to the XRD data in Fig. 4a, the interlayer distances (d) of BN were calculated from the (002) reflections by applying Bragg's law ($2d\sin\theta = n\lambda$), when $\theta = 26.62$, the calculated $d = 3.438$ Å. And diameter of N₂ is 3.64 Å ($d' = 3.64$ Å). After infiltration of L-N₂, the heated BN facilitates the instantaneous gasification of L-N₂. Then final structure of h-BN layer is tilted because of the larger size of N₂ ($d' > d$). Moreover, exfoliation process would overcome the lip-lip interaction and van der Waals force between layers. It's an endothermic process. So, the thermophilic treatment is beneficial to exfoliate. And the production yield of BN-15 with few-layered structure is about 14–18% by weight. This process is environmental and green since N₂ is an inexpensive and nontoxic reagent. Meanwhile, there are no impurities left in the product because of the evaporation of L-N₂ after exfoliation.

The adsorption behavior of BN-15 sample was investigated with the organics of TC, GT, RhB, and MB. The effect of contact time was investigated to obtain the equilibrium time. As shown in Fig. 5a, the adsorption capacities of organic contaminants increased rapidly during

the initial period of testing time. The equilibrium almost achieved within 60 min. The pseudo-first-order and pseudo-second-order kinetic models (Supplementary data, Section S1) were employed to fit the adsorption data (Table 1). The adsorption of TC, GT, RhB, and MB on BN-15 followed with the pseudo-second-order kinetic model (Fig. 5b), unraveling that the adsorption process was dependent on the surface sites of adsorbent and the amount adsorbed at equilibrium [32].

The adsorption capacities of different organic pollutants were investigated under the same condition. The results were shown in Fig. 5c. BN-15 showed much higher adsorption capacities for TC (85 mg/g), GT (107 mg/g), RhB (73 mg/g) and MB (137 mg/g) than that of Com-BN (32, 75, 33 and 74 mg/g, respectively). The significantly increased adsorption capacity may result from the higher SSA and thinner layer. The higher SSA and thinner layer caused better exposure of surface B atoms and N atoms than the bulk one, and more solutes were adsorbed on the surface of BN-15. So, we confirmed that the gas exfoliation of bulk BN could increase active sites and enhance the adsorption capacity. Furthermore, a good reusability behavior of the adsorbent was significant for the removal of organic pollutants. Owing to the superior thermal stability of BN, the adsorbents can be recycled by heating at 600 °C for 2 h in a muffle furnace to remove the adsorbed organic

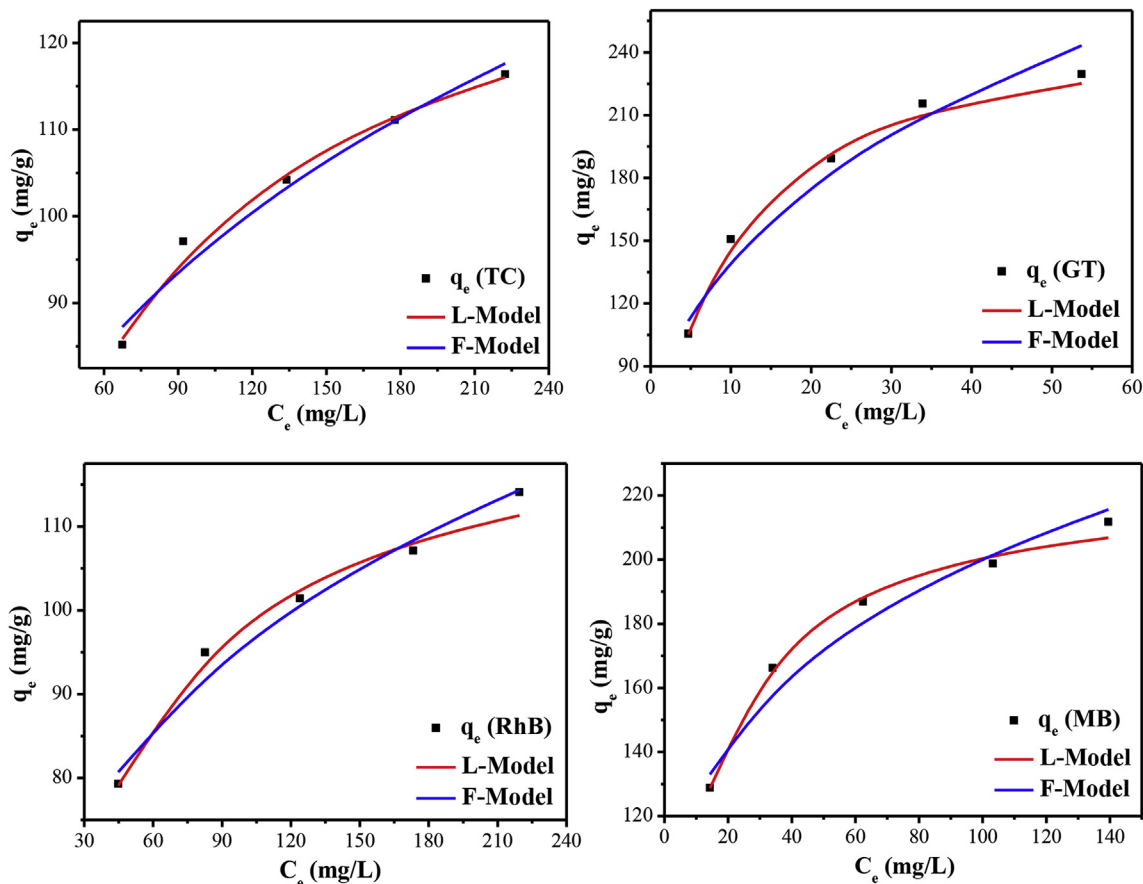


Fig. 6. Adsorption isotherms for TC, GT, RhB and MB on BN-15. (Condition: $C_0 = 100, 150, 200, 250, 300$ mg/g; $T = 298$ K; $m = 5$ mg; $V = 10$ mL; $t = 60$ min).

Table 2

Isotherm parameters of different organic pollutants adsorption on BN-15.

	Langmuir			Freundlich		
	q_m (mg/g)	K_L (L/mg)	R^2	n	K_F (L/mg)	R^2
TC	137	0.025	0.9910	3.99	30.40	0.9747
GT	252	0.15	0.9973	3.12	67.97	0.9712
RhB	124.	0.039	0.9906	4.56	35.08	0.9829
MB	222	0.096	0.9930	4.71	75.66	0.9741

pollutants. BN-15 showed excellent reusability after eight times recycling test (Fig. 5d).

The adsorption isotherms of TC, GT, RhB and MB onto BN-15 were simulated by plotting equilibrium adsorption capacity (q_e) versus equilibrium concentration of organic pollutants (C_e), respectively. Langmuir and Freundlich models (Supplementary data, Section S2) were explored to simulate the adsorption isotherms and the results were shown in Fig. 6 and Table 2. According to the correlation coefficient of the two models, experimental data were well fitted with the Langmuir model, which further suggested that the adsorption behavior was followed by the monolayer coverage. The calculated maximum adsorption capacities for TC, GT, RhB and MB onto the BN-15 were 137, 252, 124 and 222 mg/g, respectively.

4. Conclusions

In conclusion, we proposed a simple gas exfoliation method to synthesize few-layer BN, which presented an enhanced adsorption capacity to organic contaminants. More active sites associated with larger SSA and thinner layer could capture more organic contaminants. BN-15

not only possessed superior adsorption behavior but also can be reused for 8 times with a simple heat treatment. We expect this strategy can be extended to other two-dimensional materials and provides an effective approach for adsorption.

Acknowledgement

This work was financially supported by the National Natural Science Foundation of China of China (Nos. 21878133, 21722604 and 21606113), Postdoctoral Science Foundation of China (No.2017M611726, 2019M652518), Advanced Talents of Jiangsu University (No. 15JDG176).

Appendix A. Supplementary data

Supplementary data to this article can be found online at <https://doi.org/10.1016/j.ceramint.2019.06.117>.

References

- [1] K.R. Miner, J. Blais, C. Bogdal, S. Villa, M. Schwikowski, P. Pavlova, et al., Legacy organochlorine pollutants in glacial watersheds: a review, *Environ Sci-Proc Imp* 19 (2017) 1474–1483.
- [2] Y. Chen, L. Zang, G. Shen, M. Liu, W. Du, J. Fei, et al., Resolution of the ongoing challenge of estimating nonpoint source neonicotinoid pollution in the yangtze river basin using a modified mass balance approach, *Environ. Sci. Technol.* 53 (2019) 2539–2548.
- [3] S. Ledakowicz, R. Zylla, K. Pazdzior, J. Wrebiak, J. Sojka-Ledakowicz, Integration of ozonation and biological treatment of industrial wastewater from dyehouse, *Ozone: Sci. Eng.* 39 (2017) 357–365.
- [4] T.R. Barbosa, E.L. Foletto, G.L. Dotto, S.L. Jahn, Preparation of mesoporous geopolymer using metakaolin and rice husk ash as synthesis precursors and its use as potential adsorbent to remove organic dye from aqueous solutions, *Ceram. Int.* 44 (2018) 416–423.

- [5] J. Zhuang, J. Zhang, J. Pang, A. Wang, X. Wang, W. Zhu, Fabrication of pyrimidine/*g*-C₃N₄ nanocomposites for efficient photocatalytic activity under visible-light illumination, *Dyes Pigments* 163 (2019) 634–640.
- [6] Y. Chao, W. Zhu, X. Wu, F. Hou, S. Xun, P. Wu, et al., Application of graphene-like layered molybdenum disulfide and its excellent adsorption behavior for doxycycline antibiotic, *Chem. Eng. J.* 243 (2014) 60–67.
- [7] M.G. Cantwell, D.R. Katz, J.C. Sullivan, K. Ho, R.M. Burgess, Temporal and spatial behavior of pharmaceuticals in Narragansett Bay, Rhode Island, United States, *Environ. Toxicol. Chem.* 36 (2017) 1846–1855.
- [8] M. Wang, Y. Bai, B. Zhang, B. Zhong, Y. Yu, J. Zhang, et al., Large scale fabrication of porous boron nitride microrods with tunable pore size for superior copper (II) ion adsorption, *Ceram. Int.* 45 (2019) 6684–6692.
- [9] A.S. Dhmees, A.M. Rashad, A.A. Eliwa, M.F. Zawrah, Preparation and characterization of nano SiO₂@CeO₂ extracted from blast furnace slag and uranium extraction waste for wastewater treatment, *Ceram. Int.* 45 (2019) 7309–7317.
- [10] H. Li, W. Zhu, S. Zhu, J. Xia, Y. Chang, W. Jiang, et al., The selectivity for sulfur removal from oils: an insight from conceptual density functional theory, *AIChE J* 62 (2016) 2087–2100.
- [11] W. Zhu, B. Dai, P. Wu, Y. Chao, J. Xiong, S. Xun, et al., Graphene-analogue hexagonal BN supported with tungsten-based ionic liquid for oxidative desulfurization of fuels, *ACS Sustain. Chem. Eng.* 3 (2015) 186–194.
- [12] P. Wu, W. Zhu, Y. Chao, J. Zhang, P. Zhang, H. Zhu, et al., A template-free solvent-mediated synthesis of high surface area boron nitride nanosheets for aerobic oxidative desulfurization, *Chem. Commun.* 52 (2016) 144–147.
- [13] L. Lu, J. He, P. Wu, Y. Wu, Y. Chao, H. Li, et al., Taming electronic properties of boron nitride nanosheets as metal-free catalysts for aerobic oxidative desulfurization of fuels, *Green Chem.* 20 (2018) 4453–4460.
- [14] T.A. Parthasarathy, B. Cox, O. Sudre, C. Przybyla, M.K. Cinibulk, Modeling environmentally induced property degradation of SiC/BN/SiC ceramic matrix composites, *J. Am. Ceram. Soc.* 101 (2018) 973–997.
- [15] F. Guo, P. Yang, Z. Pan, X.N. Cao, Z. Xie, X. Wang, Carbon-doped BN nanosheets for the oxidative dehydrogenation of ethylbenzene, *Angew. Chem. Int. Ed.* 56 (2017) 8231–8235.
- [16] X. Yao, C. Wang, H. Liu, H. Li, P. Wu, L. Fan, et al., Immobilizing highly catalytically molybdenum oxide nanoparticles on graphene-analogous BN: stable heterogeneous catalysts with enhanced aerobic oxidative desulfurization performance, *Ind. Eng. Chem. Res.* 58 (2019) 863–871.
- [17] P. Wangyang, H. Sun, X. Zhu, D. Yang, X. Gao, Mechanical exfoliation and Raman spectra of ultrathin PbI₂ single crystal, *Mater. Lett.* 168 (2016) 68–71.
- [18] M.K. Joo, J. Kirn, J.H. Park, N. Van Luan, K.K. Kim, Y.H. Lee, et al., Large-scale graphene on hexagonal-BN Hall elements: prediction of sensor performance without magnetic field, *ACS Nano* 10 (2016) 8803–8811.
- [19] Y. Peng, Y. Li, Y. Ban, H. Jin, W. Jiao, X. Liu, et al., Metal-organic framework nanosheets as building blocks for molecular sieving membranes, *Science* 346 (2014) 1356–1359.
- [20] M.T., O.H.,K.Y., M.M.,F.K., A high-yield ionic liquid-promoted synthesis of boron nitride nanosheets by direct exfoliation, *Chem. Commun.* 51 (2015) 12068–12071.
- [21] S. Chen, R. Xu, J. Liu, X. Zou, L. Qiu, F. Kang, et al., Simultaneous production and functionalization of boron nitride nanosheets by sugar-assisted mechanochemical exfoliation, *Adv. Mater.* 31 (2019) 1804810.
- [22] H.L. Yan, P. Yu, G.C. Han, Q.H. Zhang, L. Gu, Y.P. Yi, et al., High-yield and damage-free exfoliation of layered graphdiyne in aqueous phase, *Angew. Chem. Int. Ed.* 58 (2019) 746–750.
- [23] W.S. Zhu, X. Gao, Q. Li, H.P. Li, Y.H. Chao, M.J. Li, et al., Controlled gas exfoliation of boron nitride into few-layered nanosheets, *Angew. Chem. Int. Ed.* 55 (2016) 10766–10770.
- [24] W.S. Zhu, Z.L. Wu, G.S. Foo, X. Gao, M.X. Zhou, B. Liu, et al., Taming interfacial electronic properties of platinum nanoparticles on vacancy-abundant boron nitride nanosheets for enhanced catalysis, *Nat. Commun.* 8 (2017) 15291–15298.
- [25] C. Wang, Z. Chen, X. Yao, Y. Chao, S. Xun, J. Xiong, et al., Decavanadates anchored into micropores of graphene-like boron nitride: efficient heterogeneous catalysts for aerobic oxidative desulfurization, *Fuel* 230 (2018) 104–112.
- [26] P. Wu, W. Zhu, B. Dai, Y. Chao, C. Li, H. Li, et al., Copper nanoparticles advance electron mobility of graphene-like boron nitride for enhanced aerobic oxidative desulfurization, *Chem. Eng. J.* 301 (2016) 123–131.
- [27] M. Takuya, O. Hirotsuka, K. Yoshihide, M. Mitsumasa, F. Kenzo, A high-yield ionic liquid-promoted synthesis of boron nitride nanosheets by direct exfoliation, *Chem. Commun.* 51 (2015) 12068–12071.
- [28] W. Lei, V.N. Mochalin, L. Dan, Q. Si, Y. Gogotsi, C. Ying, Boron nitride colloidal solutions, ultralight aerogels and freestanding membranes through one-step exfoliation and functionalization, *Nat. Commun.* 6 (2015) 8849.
- [29] L.H. Li, J. Cervenka, K. Watanabe, T. Taniguchi, Y. Chen, Strong oxidation resistance of atomically thin boron nitride nanosheets, *ACS Nano* 8 (2014) 1457–1562.
- [30] R.V. Gorbachev, I. Riaz, R.R. Nair, R. Jalil, L. Britnell, B.D. Belle, et al., Hunting for monolayer boron nitride: optical and Raman signatures, *Small* 7 (2015) 465–468.
- [31] R. Liu, Y. Wang, D. Liu, Y. Zou, S. Wang, Water-plasma-enabled exfoliation of ultrathin layered double hydroxide nanosheets with multivacancies for water oxidation, *Adv. Mater.* 29 (2017) 1701546.
- [32] Y. Li, C.X. Yang, X.P. Yan, Controllable preparation of core-shell magnetic covalent-organic framework nanospheres for efficient adsorption and removal of bisphenols in aqueous solution, *Chem. Commun.* 53 (2017) 2511–2514.